

## Mechanism of Catalytic Thermal Decomposition of Ammonium Perchlorate in the Presence of $Ti_3C_2T_x$

Zhanibek Korkembay<sup>1,2\*</sup>, Moldir Auyelkhanzy<sup>1,3\*\*</sup>, Meiram Atamanov<sup>3,4</sup>, Zulkhair Mansurov<sup>1,3</sup>, Viatcheslav Bykov<sup>5</sup>

<sup>1</sup>Al-Farabi Kazakh National University, 71 al-Farabi Ave., Almaty, Kazakhstan

<sup>2</sup>S.D. Asfendiyarov Kazakh National Medical University, 94 Tole Bi Str., Almaty, Kazakhstan

<sup>3</sup>Institute of Combustion Problems, 172 Bogenbay batyr Str., Almaty, Kazakhstan

<sup>4</sup>Kazakh National Women's Teacher Training University, 99, Aiteke Bi Str., Almaty, Kazakhstan

<sup>5</sup>Karlsruhe Institute of Technology (KIT), Institute of Technical Thermodynamics, Engelbert-Arnold-Str. 4, Bld. 10.91, 76131 Karlsruhe, Germany

### Article info

Received:  
13 April 2025

Received in revised form:  
27 May 2025

Accepted:  
10 July 2025

### Keywords:

Ammonium perchlorate  
MXene  
Catalysts  
Nanocomposites  
Thermal decomposition  
 $Ti_3C_2T_x$ /AP composite  
Solid rocket fuel

### Abstract

The thermal decomposition of ammonium perchlorate (AP) proceeds via a well-established stepwise mechanism. However, its catalytic decomposition under combustion conditions is not yet fully understood. This study investigates and clarifies the catalytic decomposition pathway of AP in the presence of  $Ti_3C_2T_x$ , a novel two-dimensional (2D) material with unique structural properties. MXene was chosen for its exceptional conductivity, large surface area, and layered architecture, which provide active sites for redox interactions and enhance the thermal decomposition rate of AP. During combustion of AP-based solid rocket propellants, MXene acts as a catalyst, promoting more complete and rapid oxidation reactions. The combustion products were thoroughly analyzed using X-ray phase analysis, and based on the obtained data, stoichiometric equations for the potential reaction pathways were proposed. These equations highlight the formation of metal oxides and intermediate chlorinated compounds. Furthermore, a schematic model illustrating the catalytic action of  $Ti_3C_2T_x$  was developed, showing the interaction between AP molecules and MXene's surface functional groups. These findings advance understanding of nanocatalyst behavior in energetic materials and offer insights for improving solid-propellant performance via MXene incorporation.

## 1. Introduction

Two-dimensional layered materials kindling academia's interest are widely used in various fields. 2D monolayers called MXene are composed of transition metal carbides/nitrides. MXene differs from traditional 2D materials such as graphene and phosphorus in their high electronic conductivity, surface hydrophilicity, and unique redox properties [1, 2]. These 2D carbides possess unique crystal structures and external transition metal d-orbital electrons,

which distinguish them from conventional catalysts and energy storage material [3, 4]. Experimental and theoretical studies show that electrocatalytic activity strongly depends on their structure, conductivity, extreme states, defects, tensile stress, etc. [5, 6]. Within this family,  $Ti_3C_2T_x$  has recently attracted attention in thermal catalysis. Its high thermal stability and distinctive structural features offer advantages over conventional catalysts. High thermal stability and unique structures put MXene at an advantage over traditional catalysts [7].

The unique structure of transition-metal carbides makes MXene a promising catalyst. Several recent studies have shown that this material exhibits a catalytic effect on the thermal decomposition

\*Corresponding authors.

E-mail address: [janibek\\_kk@mail.ru](mailto:janibek_kk@mail.ru)  
[auyelkhanzy@gmail.com](mailto:auyelkhanzy@gmail.com)

of AP [8, 9]. Yang et al. [8] investigated the influence of vanadium carbide ( $V_2C$ ) MXene to the combustion of AP-based propellants and established that the presence of  $V_2C$  led to decompose of AP in both direct reaction decomposition and catalytic decomposition. Tang et al. [9] investigated the influence of  $Ti_3C_2$  on combustion behavior of AP without additional any fuel and other catalyst in an open environment combustion test. Moreover, authors prepared  $Ti_3C_2/$ AP composites having a sandwich structure and different amount of  $Ti_3C_2$  by a facial freeze-drying method. Obtained  $Ti_3C_2/$ AP composites showed that its combustion is depending on content of the  $Ti_3C_2$ . For instance, at 20–40 wt% of  $Ti_3C_2$  self-sustained luminous flame with bright light emission were observed. Finally, authors found that the  $Ti_3C_2$  not only improves the pyrolysis reaction kinetics of AP based composites, but also increases the energy output of the propellants. However, this research has been considered MXene as a fuel and a catalytic effect has not been thoroughly investigated. Therefore, it is essential to clarify the catalytic mechanisms of  $Ti_3C_2T_x$  in AP decomposition [10]. In this work, a series of experiments was conducted to study the catalytic thermal decomposition of AP in solid rocket propellants containing  $Ti_3C_2T_x$ .

AP is one of the most essential oxidizing and energy materials in solid rocket fuel, which gives rockets muscular strength by releasing large amounts of heat and gases [11]. Optimization of the combustion of solid rocket fuels based on AP is of great importance in the development of powerful rocket engines. Therefore, various catalysts have been used for many years to improve AP and ammonium nitrate thermal decomposition efficiency, such as metals, metal oxides [12, 13], and carbon or carbon-based materials [14, 15]. Owing to their large surface area, unique layered structure, and excellent electrical conductivity, these 2D carbides have been employed as direct catalysts in solid propellant combustion [16–18]. Their spatial architecture with abundant active sites and hydrophilic nature also makes them highly sensitive to various gases. For instance,  $Ti_3C_2T_x$  has been tested for adsorption of  $NH_3$ ,  $H_2$ ,  $CH_4$ ,  $CO$ ,  $CO_2$ ,  $N_2$ ,  $NO_2$  and  $O_2$  [19]. Hence,  $Ti_3C_2T_x$  is a perfect nanostructured substrate that accelerates the thermal decomposition of AP during combustion. The research included preparation of samples of AP-based solid rocket fuel added with a multilayer  $Ti_3C_2T_x$  catalyst, the study of the  $Ti_3C_2T_x$  catalytic effect on thermal decomposition of AP succeeded by the analysis of solids after combustion inside the chamber.

## 2. Materials and methods

Our previous paper provided a detailed description of the preparation of  $Ti_3C_2T_x$  powders [20]. In short, the required volume of hydrofluoric acid (HF, 40%) was added to the known mass of  $Ti_3AlC_2$  (MAX phase). The mixture was gently stirred with a magnetic stirrer for 18 h at 60 °C. The resulting slurry was washed several times with deionized water and then vacuum-dried at 80 °C for 24 h.

Samples of AP-based solid rocket propellants incorporating MXene at various weight ratios (0%, 2%, 3%, and 5%) have been synthesized, then fabricated into cylindrical shapes, 15 mm high and 8 mm in diameter each. As shown in Fig. 1, the prepared samples were ignited within a high-pressure chamber under argon gas pressures of 1, 20, 40, and 60 atm. The heating process was facilitated using a nichrome spiral wire. The combustion rate was determined by dividing the height of the cylindrical samples (15 mm in length and 8 mm in diameter) by the time required for complete combustion.

To elucidate the structure and composition of the catalyst, evaluate the impact of  $Ti_3C_2T_x$  on the thermal decomposition of AP, and characterize the solid residues after combustion, the following advanced analytical techniques were employed.

Microstructural characterization of the samples was conducted using SEM, employing a Quanta 3D 200i Dual system coupled with a field emission scanning electron microscope, operating at an accelerating voltage of 15 kV. The thermal decomposition

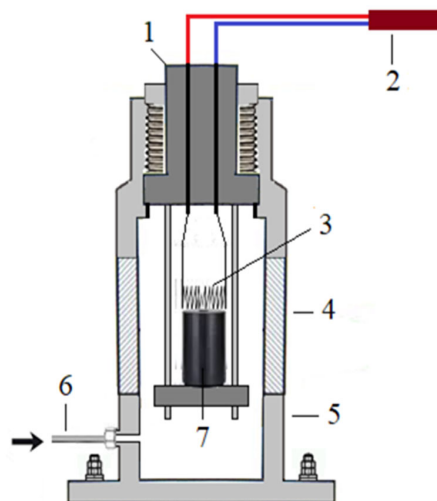


**Fig. 1.** Schematic version of the pattern on a high-pressure device: 1 – opening and closing cap; 2 – current; 3 – heating spiral; 4 – control window; 5 – pressure device; 6 – gas inlet and outlet tube; 7 – composite fuel in the shape of a cylinder.

of AP was investigated using a differential scanning calorimeter (STA 409 PC/PG, NETZSCH, Germany), and conducted under both inert and oxidizing atmospheres, with a heating rate of 10 °C/min. X-ray phase analysis was performed using a Rigaku mini-flex 600 X-ray diffractometer. It is based on a physical phenomenon – diffraction.

### 3. Results and discussion

As depicted in the SEM images (Fig. 2a and b), the  $\text{Ti}_3\text{C}_2\text{T}_x$  exhibits a surface morphology characterized by multilayered structural nanoparticles. The elemental composition of  $\text{Ti}_3\text{C}_2\text{T}_x$ , as determined by energy-dispersive X-ray (EDX) analysis (Fig. 2c), reveals the presence of Ti and C, along with trace amounts of O, F, and Al in varying proportions. The  $\text{T}_x$  termination groups which may include O, F, and Al, or combinations thereof, serve as functional surface terminations [21]. Due to its high surface-to-volume ratio, the two-dimensional structure of  $\text{Ti}_3\text{C}_2\text{T}_x$  is suitable for catalytic applications.

In analyzing the combustion of AP-based solid propellants, reference was made to the thermal decomposition data shown in Fig. 3a. A comprehensive discussion of the thermal decomposition of the  $\text{Ti}_3\text{C}_2\text{T}_x$ /AP composite is presented in our previous paper [20]. In brief, kinetic parameters, such as the apparent activation energy and exponential coefficient were determined using the Kissinger method [22]. This approach allows for the calculation of the kinetic parameters of thermal decomposition based on the values of the decomposition peaks observed in the differential thermal analysis (DTA) curve.

The DTA analysis was conducted at a heating rate of 10 °C/min, as depicted in Fig. 3b. In parallel with the percentage of  $\text{Ti}_3\text{C}_2\text{T}_x$  increase (2%, 5%, and 10%) the catalytic effect on AP diminishing takes place, mainly, due to enhanced sintering of the nanoparticles and an increase in crystal size [23]. Consequently, in the considered range the addition of 2%  $\text{Ti}_3\text{C}_2\text{T}_x$  yields the most optimal catalytic performance.

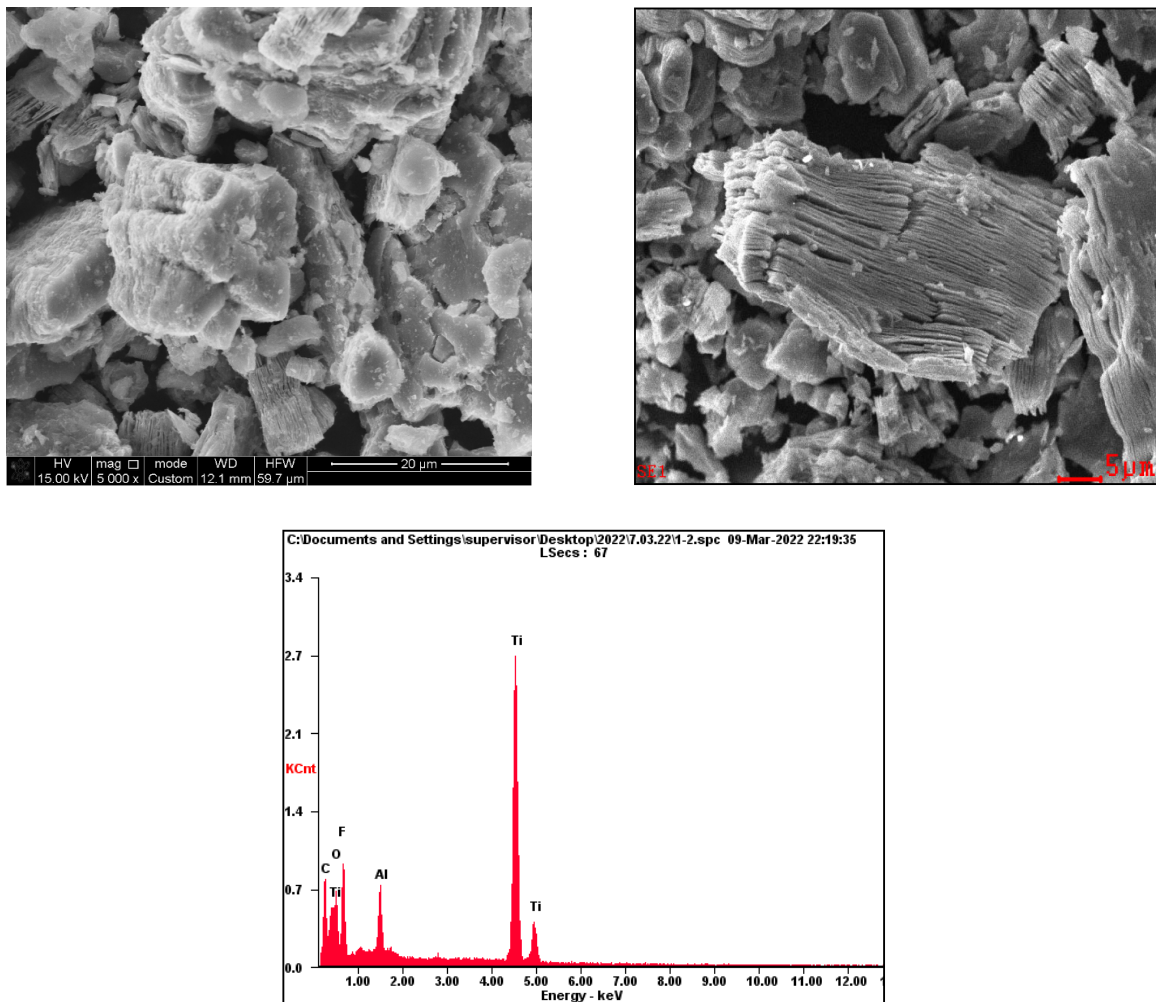


**Fig. 2.**  $\text{Ti}_3\text{C}_2\text{T}_x$  MXene's surface structure, composition and morphology: (a), (b) – SEM images, (c) – EDAX image.

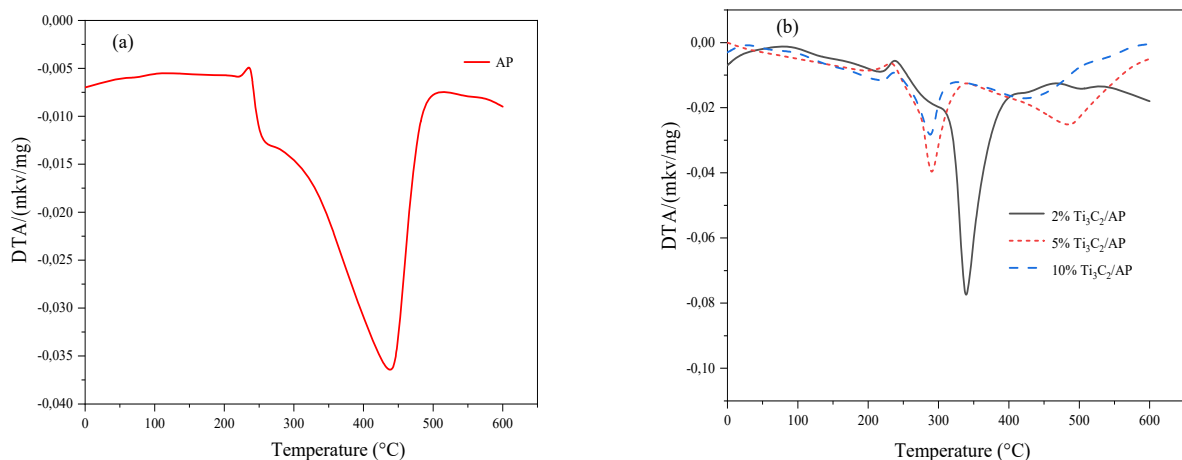


Fig. 3. AP thermal analysis DTA curves: (a) – pure AP; (b) –  $\text{Ti}_3\text{C}_2\text{T}_x$ /AP [20].

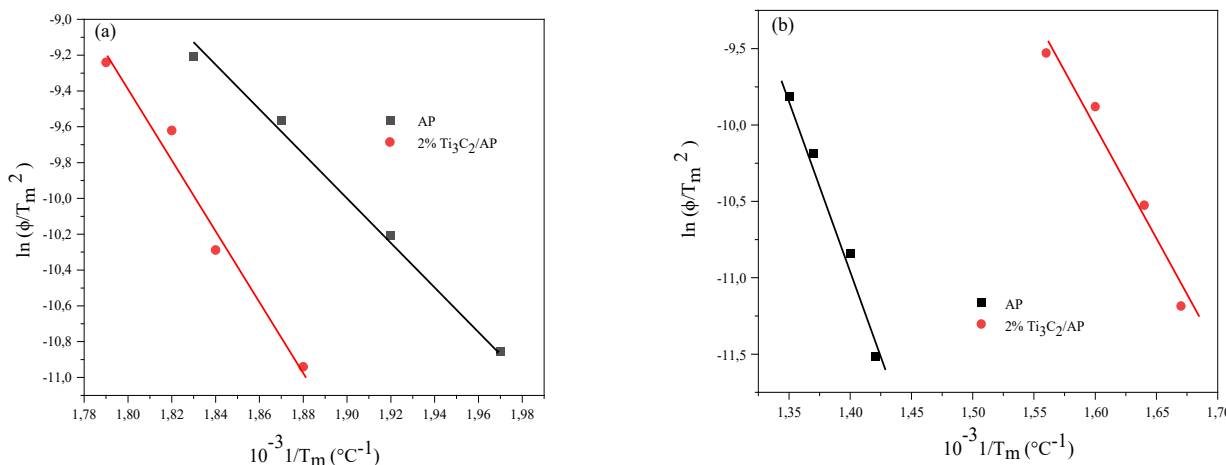


Fig. 4. Graph of activation energy during thermal decomposition of 2%  $\text{Ti}_3\text{C}_2\text{T}_x$ /AP and AP: (a) – low-temperature; (b) – high-temperature [20].

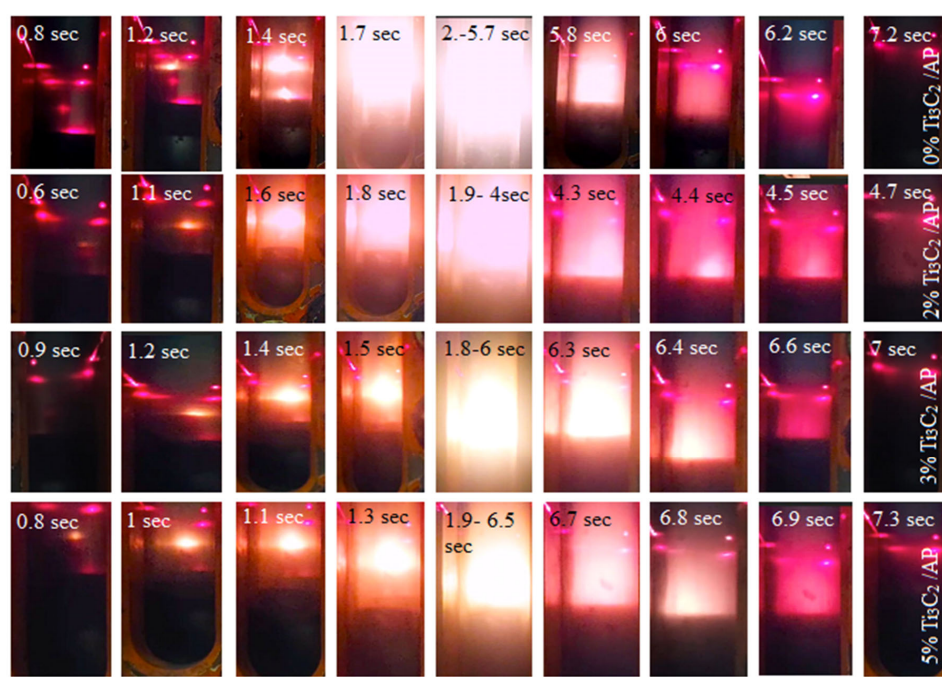
The DTA graph of composite mixture (2%  $\text{Ti}_3\text{C}_2\text{T}_x$ /AP) and of pure AP samples is obtained at a heating rate of 5; 10; 20 and 30  $^{\circ}\text{C}/\text{min}$ . Using the values at the vertices of the graph, in the Kissinger equation [18], the activation energy curve can be constructed, as shown in Fig. 4.

Figure 4 shows that presence of catalyst  $\text{Ti}_3\text{C}_2\text{T}_x$  reduces the decomposition period of AP into intermediates. However, the stage of complete decomposition occurs at a lower temperature, as compared to pure AP-thermal decomposition. This is due to a decrease in the activation energy. The decrease in activation energy allows the decomposition reaction to occur at low temperature, facilitating the combustion of AP.

Based on obtained results, it is possible to state that the 2% catalyst percentage is the most effective one, as compared to others. Figure 5 and Table 1 show the dependence of the combustion rate on the pressure, i.e. sequential increase of pressure, the

combustion surface and combustion rate. At higher chamber pressures and with an optimal catalyst fraction of the ( $\text{Ti}_3\text{C}_2\text{T}_x$ ) catalyst, the combustion rate of the composite solid fuel will increase resulting in higher energy release. Notably, as it can be seen in Table 1 the rate of combustion at different pressure levels increased by 1.5–2 mm/sec, whereas the released heat rose by 300–400  $^{\circ}\text{C}$ . The elevated combustion rate and the release of high energy could potentially enhance the operating conditions of the rocket engine [24].

The results of the X-ray phase analysis of post-combustion solid products of solid rocket fuel samples based on AP in a high-pressure device are shown in Fig. 6. According to the obtained data the primary catalyst was involved in the combustion process of  $\text{Ti}_3\text{C}_2\text{T}_x$ . As a result, substances such as  $\text{TiN}$ ,  $\text{TiO}_2$ ,  $\text{TiC}$  are formed, which accelerate the combustion rate of solid fuel.



**Fig. 5.** Combustion of composite solid fuel in a high-pressure device.

**Table 1.** Influence of pressure on combustion rate and heat dissipation

Pressure, atm	0-5% Ti <sub>3</sub> C <sub>2</sub> samples							
	0%		2%		3%		5%	
	θ, mm/sec	T <sub>(Max)</sub> °C	θ, mm/sec	T <sub>(Max)</sub> °C	θ, mm/sec	T <sub>(Max)</sub> °C	θ, mm/sec	T <sub>(Max)</sub> °C
1	1.4133	2324	1.9333	2514	1.5	2286	1.325	2015
20	1.1777	2094	1.4882	2448	1.1363	2383	0.9285	2060
40	5.0333	2862	6.1333	3193	4.6666	2933	3.9692	2870
60	6.6	3516	8.4	3820	6.075	3582	4.3666	2862

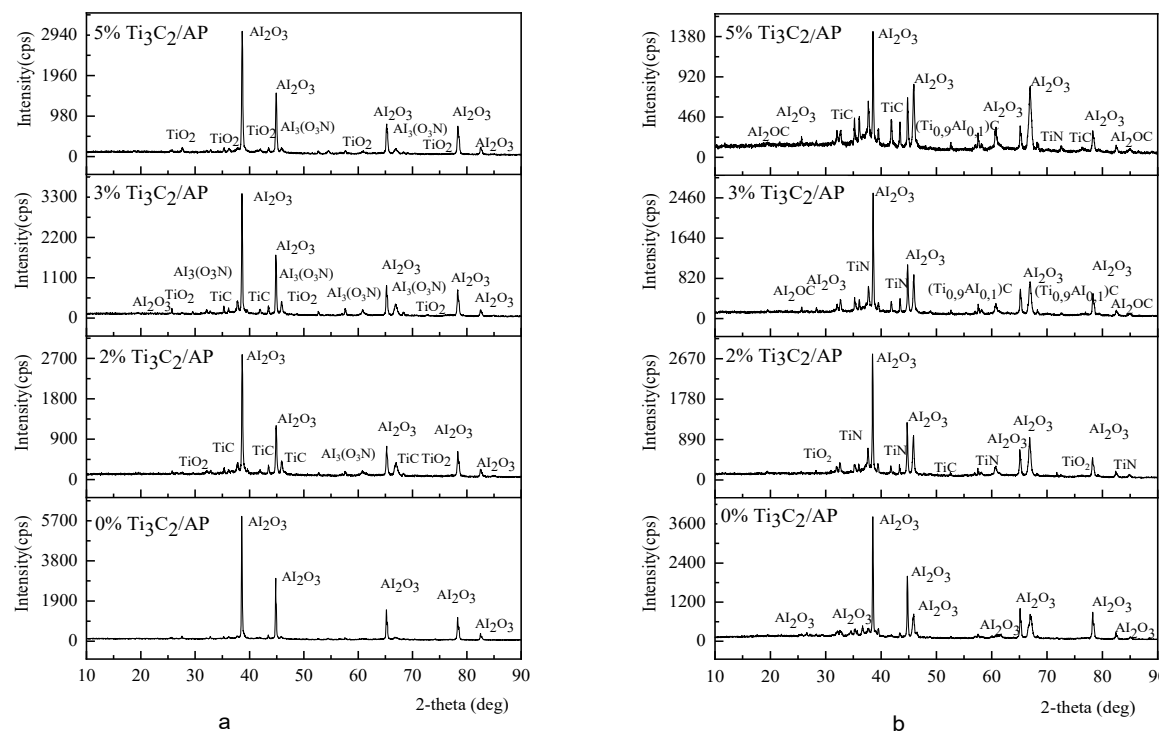
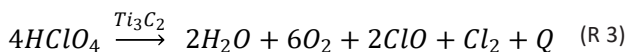
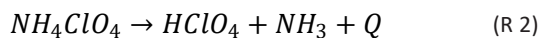
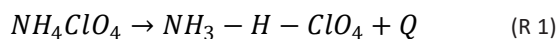


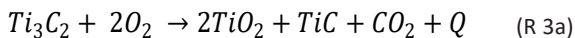
**Fig. 6.** X-ray phase analysis of the combustion products of the samples under different pressures: (a) – 1 atm; (b) – 40 atm.

This can be attributed to the link between product formation and the decomposition pathway of AP. The predicted mechanism is summarized by the stoichiometric equations given below. Because the reaction has a high activation energy, AP requires elevated temperatures to decompose, typically initiating in the range of 200–250 °C. However, this temperature range can be insufficient for complete decomposition of  $NH_4ClO_4$ , therefore the temperature can be 300–350 °C or higher. The reaction between  $Ti_3C_2$  and  $O_2$  takes place at a temperature of 600–1000 °C or higher. Since this reaction is exothermic and forms titanium dioxide and carbon dioxide through the combination of oxygen, it requires very high temperatures. The reaction between  $TiO_2$  and NO is possible in the temperature range of 700–1000 °C. High temperature is required for a stable and effective reaction.

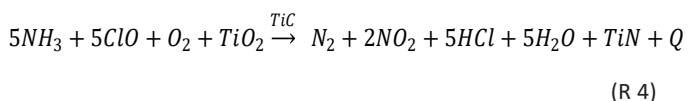
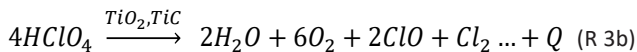
In general, the combustion of AP in composite solid fuel in the presence of  $Ti_3C_2T_x$  can be described as



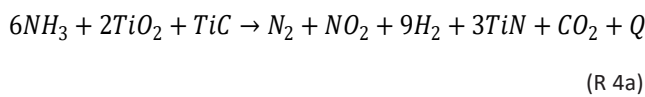
As a result of the exothermic interactions shown above, the temperature of the reaction zone rises, which causes the redox reaction of  $Ti_3C_2T_x$ , as shown below.



The products ( $TiO_2$ ,  $TiC$ ) formed continue catalyze  $HClO_4$  decomposition



At high-temperatures,  $TiO_2$ ,  $TiC$  and  $NH_3$  partially react to form



As follows from Reaction 1 of AP thermal decomposition, soon after the formation of the intermediate molecular complex  $HClO_4$ ,  $NH_3$ , decomposes as shown in Reaction 2. Chloric acid continues to decompose in the presence of the catalyst, releasing heat and increasing the temperature of the reaction zone. At this high temperature,  $TiO_x/C$  nanosheet materials are formed through a redox reaction of  $Ti_3C_2T_x$ , as shown in Reaction 3a. The  $TiO_x/C$  products perform an excellent catalytic function in the thermal decomposition of AP at high temperatures (Reactions 3b and 4). At the maximum temperature separation during the full decay period  $TiO_x/C$  and  $NH_4$  partially react to form  $TiN$  (Reaction 4a). Complete decay of AP forms  $O_2$ ,  $N_2$ ,  $N_2O$ ,  $NO$ ,  $NO_2$ ,  $HCl$ ,  $Cl_2$ ,  $H_2O$  by replacing protons. The products ( $TiC$ ,  $TiO_2$ ,  $TiN$ ), formed by oxidation of  $Ti_3C_2T_x$  during AP combustion in solid rocket fuels become active catalysts that further accelerate the thermal decomposition of AP.

#### 4. Conclusion

The proposed catalytic thermal decomposition mechanism of AP incorporates the addition of  $Ti_3C_2T_x$ , a compound known for its exceptional thermal and reactive properties. This mechanism involves four primary and three secondary reactions, illustrating the multifaceted role MXene plays in enhancing AP decomposition. As temperature increases in the reaction zone,  $Ti_3C_2T_x$  acts as a catalyst, promoting the breakdown of intermediate AP decomposition products. Simultaneously, it engages in reactions with the MXene's own decomposition product-chloric acid—thereby generating additional heat that feeds back into the overall decomposition process. This chain of reactions leads to the formation of solid-state products such as titanium carbide, titanium dioxide, and titanium nitride. These products are instrumental in further reducing the activation energy required for AP decomposition. Lower activation energy directly translates to a reduced threshold of thermal input, thereby accelerating the reaction rate and increasing the combustion intensity of the composite solid fuel. This enhancement in thermal behavior not only improves energy output but also contributes to the efficiency and reliability of propellant performance.

#### References

- [1]. M. Ryabicheva, Y. Zhigalenok, M. Skakov, et al., MXene-Based Electrocatalysts for Alkaline Water Electrolysis: a Review, *Eurasian Chem.-Technol. J.* 27 (2025) 71-88. DOI: 10.18321/ectj1656

[2]. A.S. Berkinbayeva, M. Nazhipkyzy, M. Hashami, et al., The Significant Role of Mxene's Derivatives and Composites in Supercapacitors: A Review, *ES Energy Environ.* 27 (2025) 1422. DOI: [10.30919/ee1422](https://doi.org/10.30919/ee1422)

[3]. K. Chandrasekar, S. Sudhakar, R. Rajappan, et al., Present developments and the reach of alternative fuel: A review, *Mater. Today: Proc.* 51 (2022) 74-83. DOI: [10.1016/j.matpr.2021.04.505](https://doi.org/10.1016/j.matpr.2021.04.505)

[4]. O. Salim, K. Mahmoud, K.K. Pant, R.K. Joshi, Introduction to MXenes: synthesis and characteristics, *Mater. Today Chem.* 14 (2019) 100191. DOI: [10.1016/j.mtchem.2019.08.010](https://doi.org/10.1016/j.mtchem.2019.08.010)

[5]. C.S. Lim, S.M. Tan, Z. Sofer, M. Pumera, Impact Electrochemistry of Layered Transition Metal Dichalcogenides, *ACS Nano* 9 (2015) 8474-8483. DOI: [10.1021/acsnano.5b03357](https://doi.org/10.1021/acsnano.5b03357)

[6]. T.-Y. Chen, Y.-H. Chang, C.-L. Hsu, et al., Comparative study on MoS<sub>2</sub> and WS<sub>2</sub> for electrocatalytic water splitting, *Int. J. Hydrog. Energy* 38 (2013) 12302-12309. DOI: [10.1016/j.ijhydene.2013.07.021](https://doi.org/10.1016/j.ijhydene.2013.07.021)

[7]. A.A. Mayyahi, S. Sarker, B.M. Everhart, et al., Synthesis of ultrathin, nano-sized Ti<sub>3</sub>C<sub>2</sub>T<sub>x</sub> with abundant =O and -OH terminals and high transparency as a co-catalyst: Enabling design of high-performance Titania-Ti<sub>3</sub>C<sub>2</sub>T<sub>x</sub> hybrid photocatalysts, *J. Phys. Chem. Solids* 170 (2022) 110875. DOI: [10.1016/j.jpcs.2022.110875](https://doi.org/10.1016/j.jpcs.2022.110875)

[8]. B. Yang, P-f. Tang, R. Li, et al., Reaction-dominated combustion control of ammonium perchlorate-based composites by layered V<sub>2</sub>C MXene, *Energ. Mater. Front.* 3 (2022) 199-208. DOI: [10.1016/j.enmf.2022.06.001](https://doi.org/10.1016/j.enmf.2022.06.001)

[9]. P. Tang, B. Yang, R. Li, et al., Ti<sub>3</sub>C<sub>2</sub> MXene: A reactive combustion catalyst for efficient burning rate control of ammonium perchlorate based solid propellant, *Carbon* 186 (2022) 678-687. DOI: [10.1016/j.carbon.2021.10.069](https://doi.org/10.1016/j.carbon.2021.10.069)

[10]. J. Li, Y. Du, X. Wang, X. Zhi, Enhanced Catalytic Effect of Ti<sub>2</sub>CT<sub>x</sub>-MXene on thermal decomposition behavior of ammonium perchlorate, *Materials* 16 (2023) 344. DOI: [10.3390/ma16010344](https://doi.org/10.3390/ma16010344)

[11]. D. Yang, W. Mo, S. Zhang, et al., A graphene oxide functionalized energetic coordination polymer possesses good thermostability, heat release and combustion catalytic performance for ammonium perchlorate, *Dalton Trans.* 49 (2020) 1582-1590. DOI: [10.1039/C9DT03491A](https://doi.org/10.1039/C9DT03491A)

[12]. M.A. Fertassi, K.T. Alali, Q. Liu, et al., Catalytic effect of CuO nanoplates, a graphene (G)/CuO nanocomposite and an Al/G/CuO composite on the thermal decomposition of ammonium perchlorate, *RSC Adv.* 6 (2016) 74155-74161. DOI: [10.1039/C6RA13261H](https://doi.org/10.1039/C6RA13261H)

[13]. L. Zhou, S. Cao, L. Zhang, et al., Facet effect of Co<sub>3</sub>O<sub>4</sub> nanocatalysts on the catalytic decomposition of ammonium perchlorate, *J. Hazard. Mater.* 392 (2020) 122358. DOI: [10.1016/j.jhazmat.2020.122358](https://doi.org/10.1016/j.jhazmat.2020.122358)

[14]. J. Chen, B. Huang, Y. Liu, et al., 3D Hierarchically ordered porous carbon entrapped Ni nanoparticles as a highly active catalyst for the thermal decomposition of ammonium perchlorate, *Energ. Mater. Front.* 2 (2021) 14-21. DOI: [10.1016/j.enmf.2021.01.003](https://doi.org/10.1016/j.enmf.2021.01.003)

[15]. Z.A. Mansurov, M.K. Atamanov, Z. Elemesova, et al., New Nanocarbon High-Energy Materials, *Combust. Explos. Shock Waves* 55 (2019) 402-408. DOI: [10.1134/S0010508219040051](https://doi.org/10.1134/S0010508219040051)

[16]. K. Li, Y. Lei, J. Liao, et al., Design of three dimensional flower-like MXene/manganese-cobalt spinel nanocomposites for efficient catalytic thermal decomposition of ammonium perchlorate, *Ceram. Int.* 47 (2021) 33269-33279. DOI: [10.1016/j.ceramint.2021.08.228](https://doi.org/10.1016/j.ceramint.2021.08.228)

[17]. L. Tan, J. Lv, X. Xu, et al., Construction of MXene/NiO composites through in-situ precipitation strategy for dispersibility improvement of NiO nanoparticles, *Ceram. Int.* 45 (2019) 6597-6600. DOI: [10.1016/j.ceramint.2018.12.114](https://doi.org/10.1016/j.ceramint.2018.12.114)

[18]. L. Zhu, J. Lv, X. Yu, et al., Further construction of MnO<sub>2</sub> composite through In-situ growth on MXene surface modified by carbon coating with outstanding catalytic properties on thermal decomposition of ammonium perchlorate, *Appl. Surf. Sci.* 502 (2020) 144171. DOI: [10.1016/j.apsusc.2019.144171](https://doi.org/10.1016/j.apsusc.2019.144171)

[19]. X. Yu, Y. Li, J. Cheng, et al., Monolayer Ti<sub>2</sub>CO<sub>2</sub>: A Promising Candidate for NH<sub>3</sub> Sensor or Capturer with High Sensitivity and Selectivity, *ACS Appl. Mater. Interfaces* 7 (2015) 13707-13713. DOI: [10.1021/acsami.5b03737](https://doi.org/10.1021/acsami.5b03737)

[20]. Zh. Korkembay, K. Toshtay, M. Atamanov, et al., Determination of the Catalytic Activity of the MXene in the Combustion of Ammonium Perchlorate, *J. Eng. Phys. Thermophys.* 97 (2024) 985-992. DOI: [10.1007/s10891-024-02968-1](https://doi.org/10.1007/s10891-024-02968-1)

[21]. T.A. Oyehan, B.A. Salami, A.A. Abdulrasheed, et al., MXenes: Synthesis, properties, and applications for sustainable energy and environment, *Appl. Mater. Today* 35 (2023) 101993. DOI: [10.1016/j.apmt.2023.101993](https://doi.org/10.1016/j.apmt.2023.101993)

[22]. Y. Zhang, A. Song, D. Ma, M. Ma, The catalytic decomposition and kinetic analysis of ammonium perchlorate on MgO nanoflakes, *J. Phys. Chem. Solids* 157 (2021) 110205. DOI: [10.1016/j.jpcs.2021.110205](https://doi.org/10.1016/j.jpcs.2021.110205)

[23]. M.W. Evans, R.B. Beyer, L. McCulley, Initiation of Deflagration Waves at Surfaces of Ammonium Perchlorate-Copper Chromite-Carbon Pellets, *J. Chem. Phys.* 40 (1964) 2431-2438. DOI: [10.1063/1.1725544](https://doi.org/10.1063/1.1725544)

[24]. S.S. Joshi, P.R. Patil, V.N. Krishnamurthy, Thermal decomposition of ammonium perchlorate in the presence of nanosized ferric oxide, *Defence Sci. J.* 58 (2008) 721-727. DOI: [10.14429/dsj.58.1699](https://doi.org/10.14429/dsj.58.1699)